

Role of the Electrode Potential in the Charge-Transfer Mechanism of Surface-Enhanced Raman Scattering

Juan F. Arenas, David J. Fernández, Juan Soto, Isabel López-Tocón, and Juan C. Otero*

Department of Physical Chemistry, Faculty of Sciences, University of Málaga, E-29071-Málaga, Spain

Received: July 14, 2003; In Final Form: September 22, 2003

A general model concerning the role of the electrode potential on the charge-transfer enhancement mechanism of SERS is proposed, justifying the existence of a parameter β which reduces the effectiveness of the electrode potential in order to shift the excited charge-transfer level. This explains the observed deviation of β from the unity, and allows for relating the intensity/electrode-potential (SERS–CT) profiles of similar adsorbates with the respective electron affinities. The SERS of pyridine, pyrazine and methylpyrazines have been recorded on silver, being found that the electrode potential in the maximum of the SERS–CT profiles shifts toward more negative values as the number of methylsubstituents attached to the pyrazine ring increases. This result has been explained on the basis of the relative stability of the radical anions given that a correlation between those shifts and the calculated *ab initio* vertical transition energies between the neutral molecules and their respective radical anions can be established. This confirms the participation of a resonant charge-transfer mechanism in the SERS as well as the usefulness of this technique to gain insight into the electronic properties of the doublet states of the here studied molecules.

Introduction

The origin of the enhancement of surface-enhanced Raman scattering (SERS) has been widely controversial since its discovery, and the presence of the charge-transfer (CT) mechanism has been under discussion for the last 25 years.^{1,2} Despite that, sufficient experimental evidence has been accumulated to confirm the importance of its contribution to the SERS phenomenon.³ Our group has developed a methodology to determine whether a CT mechanism is present in any particular SERS and to analyze the spectra conveniently.^{4,5} Our aim in this field is to make evident the main role of the CT enhancement in SERS and to demonstrate the usefulness of these spectra in studying the radical anions of molecules structurally similar to those studied here. These anions correspond to doublet states of benzene, pyridine, pyrazine, and so forth and are not very well known.

In a series of previous papers, we explained the SERS enhancement of totally symmetric modes of pyrazine,^{4a} pyridine,^{4b,e} and methyl derivatives^{4c–h} on the basis of the CT mechanism. In a recently published paper,⁵ we demonstrated that a CT mechanism analogous to that in resonance Raman (RR) can account for the activity of every observed band in the SERS spectra of pyrazine, even in the case of very weak nontotally symmetric fundamentals as well as for its dependence on the electrode potential. The whole analysis has been done exclusively on the basis of differences between the *ab initio* calculated properties of the potential energy surfaces (geometries^{4,5} and frequencies⁵) of the neutral molecules and their respective radical anions.

In this work, the effect of the electrode potential on the resonant charge-transfer mechanism of SERS is discussed. Unlike the above-mentioned cases where the SERS of each species has been studied separately, we discuss for the first time

the comparative behavior of the SERS of eight aromatic molecules, namely, pyrazine, its six methyl derivatives, and pyridine. The observed differences have been explained on the basis of the relative stability of the respective radical anions. The stability of an anion is related to the energy of the vertical transition E_{ver} between the ground electronic states of the neutral molecule ($A;S_0$) and its anion, which is named $A^-;D_0$ given that it is a doublet. By defining $E_{\text{ver}}(D_0 - S_0)$, the anion will be less stable because the difference between the energies of both states is more positive, in a similar way to the electron affinity (EA) but with the opposite sign.⁶ These vertical transitions E_{ver} can be estimated by *ab initio* calculations. Finally, the results of pyrazine are taken as a reference to establish a scale of relative stability for the anions of the studied molecules.

As we shall show, when the energy of the photon ($h\nu$) is kept constant the electrode potential corresponding to the maximum of the intensity/electrode-potential profiles of the SERS bands shifts toward more negative electrode potential values as the number of methyl substituents in the ring of pyrazine increases. This indicates that the respective anions become less stable with respect to the neutral molecule as the methylation proceeds. This result agrees with the *ab initio* calculated energies of the radical anions and the neutral molecules. This correlation is a new step in the understanding of the SERS phenomenon and allows us to stress the usefulness of this technique to study CT processes.

Experimental Section and Computational Details

Pyridine and liquid methylpyrazines (Aldrich) were purified by vacuum distillation before recording their spectra, and pyrazine and tetramethylpyrazine (Aldrich) were purified by sublimation. SERS spectra were recorded *in situ* using a three-electrode cell controlled by a PAR#173/175 electrochemical system. The auxiliary electrode is Pt (Metales Preciosos), and every potential is in reference to a saturated KCl/AgCl/Ag

* Corresponding author. E-mail: jc_otero@uma.es. Fax: +34 952132047.

reference electrode (PAR#K0260). The pure Ag (Metales Preciosos) working electrode has been polished with 1.0-, 0.3- and 0.05- μm alumina (Büeler) before recording the SERS; then it has been roughened by keeping the electrode at -0.5 V and subjecting it to 10 2-s pulses at $+0.6$ V in a 0.1 M KCl aqueous solution by using degassed, deionized, triply distilled water. SERS of the different samples were recorded at several electrode potentials from 0.1 M solutions in aqueous 0.1 M KCl. We used a Jobin-Yvon U-1000 Raman spectrometer fitted with a Hamamatsu PMT 943-03 photomultiplier by using the 514.5-nm exciting line from a Spectra Physics 2020 Ar⁺ laser with an effective power of 30 mW reaching the sample.

The RHF/6-31++G energies of the neutral molecules as well as the UHF energies of the respective radical anions have been computed by using the Gaussian 94 program.⁷ The spin contamination of the unrestricted calculations can be seen as moderate,⁵ the expectation value of the $\langle S^2 \rangle$ operator being <0.84 .

Results and Discussion

I. RR-CT Model. The background to analyze the SERS spectra has been described extensively in refs 4 and 5. Briefly, the charge-transfer mechanism of SERS is considered to be analogous to the RR mechanism (RR-CT). In RR, molecule A is photoexcited up to a stationary state (A^*), usually the first excited singlet S_1 . The resonance condition is tuned by the energy of the laser photon ($h\nu$), and the position of the maximum ($h\nu_{\text{max}}$) in the Raman excitation profiles (REP)⁸ relates to the energy of the vertical transition between the S_1 and S_0 states, $E_{\text{ver}}(S_1 - S_0) = h\nu_{\text{max}}$.

The main difference between the RR and RR-CT mechanisms is that in the latter the transient excited state corresponds to a charge-transfer (CT) state of the metal-adsorbate complex similar to that observed in some inorganic CT complexes.¹ In SERS, such new electronic CT transitions originate from photoinduced charge donation from the metal surface to the adsorbate or vice versa and have been detected in very few cases.⁹ Given that the available information about these CT states is quite scarce, we have proposed a simplified RR-CT mechanism that is based on the following steps. Step 1: The molecule from which the SERS is recorded (A) should be directly linked to the metal (M), which in turn is at a particular electric potential, thus giving rise to a surface complex $M-A$. Step 2: If the energy of the photon matches that of the CT transition ($h\nu = E_{\text{ver}}(\text{CT} - S_0)$, where CT and S_0 are the excited and the ground states of the surface complex, respectively), then a resonant CT process occurs. Step 3: In molecules that are similar to the ones studied here, the donated charge amounts to a complete electron in the CT state being transferred initially from the metal to the adsorbate,¹⁰ yielding the formation of the adsorbate anion in the CT excited level M^+-A^- .

These steps are supported by several experimental facts.¹ In step 3, the relative intensities observed in the SERS of several adsorbates are strictly compatible with the differences between the electronic properties of the neutral molecules and their respective radical anions.^{4,5} In step 2, the energies of the visible photons commonly used in Raman are in the range of the experimental energies of the CT transitions.⁹ In step 1, the shifts detected between the vibrational frequencies of the Raman and the SERS spectra confirm the formation of surface complex $M-A$. In the molecules studied here, these shifts originate from the adsorption through the lone electron pair of one of the nitrogen atoms of the aromatic ring, which implies a perpendicular orientation of the adsorbate with respect to the metal

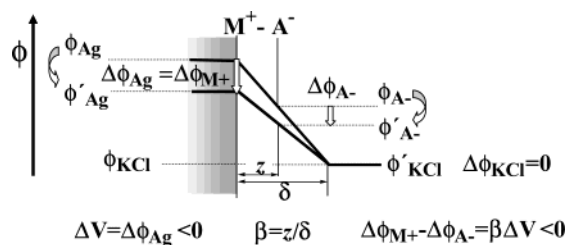


Figure 1. Dependence of the electric potential at the positions of M^+ ($\Delta\phi_{M^+}$) and A^- ($\Delta\phi_{A^-}$) species on the electrode potential (ΔV).

surface over the whole studied range of electrode potentials.^{5,11,12} Moreover, these frequency shifts, although significant, are rather small at any electrode potential, thus pointing out that the adsorption is not very strong. Therefore, we assume that the properties of the adsorbate in the ground ($M-A$) as well as in the CT state (M^+-A^-) of the surface complex are similar to those in the corresponding isolated species $A;S_0$ and $A^-;D_0$, respectively, at any electrode potential. All of these hypothesis have been confirmed in recent work in which the properties of the ground state and the excited electronic states of the Ag_2 -pyrazine complex have been studied.^{11b,13}

The energy of CT transitions $E_{\text{CT}}(\text{CT} - S_0) = E_{\text{CT}}(M^+-A^- - MA)$ depends on the work function of the solvated metal in the presence of the adsorbate Φ_M on the electron affinity of the adsorbate measured in the gas phase, EA_A , on the adsorption and partial solvation energies of species A and A^- , H_A and H_{A^-} , respectively,⁶ on the interaction between the positive charge of the metal M^+ and the negative charge of the anion A^- with the electric potential of the interphase in the position of such species, $e\phi_{M^+}$ and $-e\phi_{A^-}$, respectively, and on the electrostatic interaction between both charged species $-e^2/z$,¹⁴ where z is the distance between the charge centers:

$$E_{\text{CT}} = \Phi_M + H_{A^-} - H_A - EA_A + e(\phi_{M^+} - \phi_{A^-}) - \frac{e^2}{z} \quad (1)$$

Dependence of E_{CT} on the Electrode Potential. The role of the electrode potential is just to tune the energy of the CT transition E_{CT} . The difference ($\phi_{M^+} - \phi_{A^-}$) is not experimentally measurable, and the goal is to relate it to the electrode potential $V = \phi_{\text{Ag}} - \phi_{\text{Ag,ref}}$, which includes the potential difference at the working electrode ($\phi_{\text{Ag}} - \phi_{\text{KCl}}$). To clarify this relationship let us propose a simple example as shown in Figure 1, where a linear decay of the electric potential is assumed to take place in the Ag/KCl interphase with a width of $\delta \geq z$. Under such conditions,

$$\beta = \frac{\phi_{M^+} - \phi_{A^-}}{\phi_{\text{Ag}} - \phi_{\text{KCl}}} = \frac{z}{\delta} < 1 \quad (2)$$

When the electrode potential is changed from V to $V' = V + \Delta V$, ΔV equals the change in the potential of the polarizable electrode (i.e., the working electrode $\Delta V = \Delta\phi_{\text{Ag}} - \Delta\phi_{\text{KCl}}$). Figure 1 shows a case in which $\Delta V < 0$, which stabilizes species M^+ ($e\Delta\phi_{M^+} < 0$ given that $\Delta\phi_{M^+} < 0$) and destabilizes species A^- ($-e\Delta\phi_{A^-} > 0$ given that $\Delta\phi_{A^-} < 0$). In this example where the potential varies linearly, CT level M^+-A^- is stabilized by as much as $e\beta\Delta V$ with respect to the ground state when the electrode potential is changed by ΔV . If we assume that z and all of the effects of solvation and adsorption are independent of V , then

$$\Delta E_{\text{CT}}(\Delta V) = e(\Delta\phi_{M^+} - \Delta\phi_{A^-}) = e\beta\Delta V \quad (3)$$

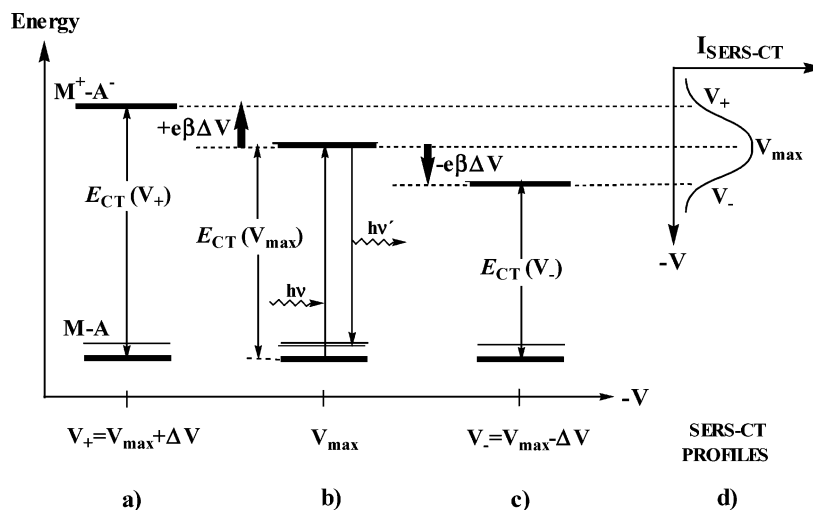


Figure 2. Dependence of the energy of the CT level ($E_{CT}(V)$) on the electrode potential (V) in the RR-CT mechanism of SERS.

Therefore, one can achieve the resonance condition in the RR-CT model by tuning the electrode potential. The origin of the SERS-CT profiles is shown in Figure 2; the plot of the intensity of a SERS band versus the electrode potential should be similar to REP, and the electrode potential of the maximum of these SERS-CT profiles (V_{max}) must be related to the energy of the vertical CT transition. The particular situation where the electrode potential has been selected to achieve the resonance condition ($E_{CT}(V_{max}) = hv$) can be seen in Figure 2b.

Dependence of V_{max} on the Energy of the Photon. Equation 3 predicts an important difference between the effect of the photon energy on RR and the electrode potential on the RR-CT mechanism of SERS. In the particular case plotted in Figure 1, with a linear variation of the electric potential of the interphase, the effectiveness of the electrode potential in shifting the CT level is reduced if $\beta < 1$. If another exciting line is used, then the energy difference between both photons does not necessarily equal the difference between the maxima of the respective profiles, given that they are related through the relationship

$$(hv_1 - hv_2) = e\beta(V_{max,1} - V_{max,2}) \quad (4)$$

An expression analogous to eq 4 has been previously used^{10,15} to deduce resonant CT processes in SERS by defining an empirical parameter S as follows:

$$S = \frac{e}{h} \frac{dV_{max}}{d\nu} = \frac{e}{h} \frac{V_{max,1} - V_{max,2}}{\nu_1 - \nu_2} \quad (5)$$

S is related to parameter β , which is introduced here, by the relationship $\beta = S^{-1}$. The most important goal of the present work is to propose a more general model for the role of the electrode potential in SERS that can explain the observed deviation of β (or S) from unity^{10,15} and can relate the SERS-CT profiles of similar adsorbates to the respective electron affinities through β .

Dependence of E_{CT} on the Electron Affinity of the Adsorbate. A direct consequence of the RR-CT model is to relate the V_{max} values of two different molecules obtained under the same experimental conditions with the relative stabilities of their respective anions. When similar molecules are dealt with, one can again assume that z and the effects due to solvation and adsorption are similar.¹⁶ Therefore, the respective V_{max} values

TABLE 1: Calculated HF/6-31++G Vertical Transitions ($E_{ver}(D_0 - S_0)$) between the Neutral Molecules (S_0 State: Restricted Calculations) and Their Respective Radical Anions (D_0 State: Unrestricted Calculations) and Experimental Electron Affinities (EA) of Benzene and Selected Azines

molecule	$E_{ver}(D_0 - S_0)$ eV	EA eV ^a
benzene	2.49	-1.14
pyridine	1.80	-0.62
pyridazine	0.99	0.25
pyrimidine	1.27	0.00
s-triazine	0.92	0.45
pyrazine	0.99	0.40

^a From ref 6.

should be related to the electron affinities as follows:

$$(EA_A - EA_B) = e\beta(V_{max,A} - V_{max,B}) \quad (6)$$

Electron Affinities and ab Initio Energies. Unfortunately, no experimental data on the effect of the methylation on the EA of methylpyrazines are available, but ab initio energy calculations have been widely used to provide valuable estimations of related magnitudes such as $E_{ver}(D_0 - S_0)$:¹⁷

$$EA_A = -E_{ver,A}(D_0 - S_0) \quad (7)$$

Table 1 summarizes the experimental EA of benzene, pyridine, pyridazine, pyrimidine, s-triazine, and pyrazine as well as the respective HF/6-31++G calculated energies of the vertical transitions $E_{ver}(D_0 - S_0)$. Despite the uncertainty in the experimental values, Figure 3 shows that the correlation between both series of values is quite satisfactory ($EA = -1.02E_{ver} + 1.33 \text{ eV} \cong -E_{ver} + 1.33 \text{ eV}$). Therefore, we derive eq 8:

$$(E_{ver,A} - E_{ver,B}) \cong -e\beta(V_{max,A} - V_{max,B}) \quad (8)$$

Dependence of E_{CT} on the Nature of the Metal. This SERS-CT simplified model can also account for the influence of the nature of the metal. For instance, in Creighton's work¹⁸ one can see that the SERS of pyridine recorded on copper sol shows SERS-CT features and that the SERS recorded on either silver or gold sols do not show CT enhancement at all. In the latter cases, the energy of the incoming photon does not afford the CT state (Figure 2a), but in the case of copper, it does indeed (Figure 2b). This is essentially due to $(\phi_{Cu} - \phi_{solution})$ being

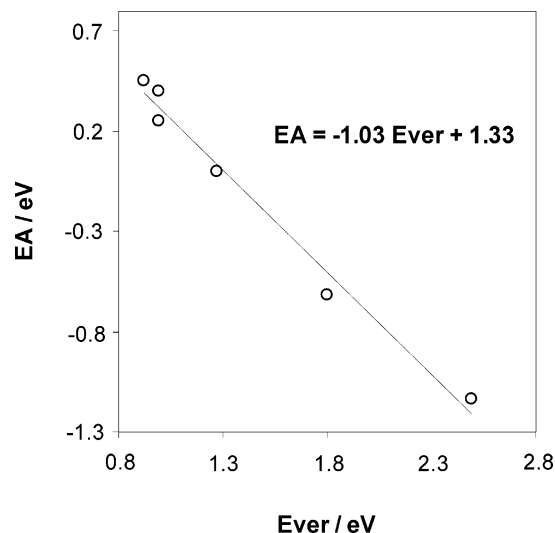


Figure 3. Correlation between the calculated energies (HF/6-31++G) of the vertical transitions ($E_{\text{ver}}(D_0 - S_0)$) and the experimental electron affinities (EA) of benzene and selected azines.

more negative in copper sol than in either gold or silver because of excess of BH_4^- , but the respective work functions may affect it too. If we assume again that all of the aforementioned approximations are valid for two different metals, then

$$(\Phi_{M1} - \Phi_{M2}) = -e\beta(V_{\text{max},M1} - V_{\text{max},M2}) \quad (9)$$

which means that the greater Φ_M is, the more negative the electrode potential should be to get the CT resonant condition.

II. SERS-CT Profiles: Intensity/Electrode-Potential Profiles. The comparison between the SERS of pyridine, pyrazine, and its six methyl derivatives (2-methyl; 2,3-, 2,5-, and 2,6-dimethyl; trimethyl; and tetramethylpyrazine) has been possible thanks to the particular features shown by the bands assigned to the $8a; \nu_{\text{ring}}$ and $\nu(\text{CH})$ vibrations, which are representative of active and inactive modes in a SERS-CT process, respectively.^{4,5,13} Generally speaking, one accepts that the most enhanced Raman vibrations in resonant conditions relate to the differences between the equilibrium structures of the involved resonant electronic states.⁸ This is the well-known Tsuboi rule,¹⁹ which accounts for the enhancement of the totally symmetric modes in RR (A term). For instance, pyrazine exhibits five totally symmetric vibrations, and in previous work we have found that the enhancement shown in SERS by four of those fundamentals, namely, $8a; \nu_{\text{ring}}$, $9a; \delta(\text{CH})$, $1; \nu_{\text{ring}}$, and $6a; \delta_{\text{ring}}$ (Figure 4a), can be quantitatively explained on the basis of the mentioned RR-CT resonant mechanism.⁵ It could be shown that the enhancement of these four fundamentals is closely related to the differences between the ab initio optimized geometries of the neutral molecule (S_0) and the respective radical anion (D_0). On the contrary, the fifth totally symmetric fundamental, $2; \nu(\text{CH})$, is inactive in this mechanism because the transferred electron is essentially located in the aromatic ring; therefore, the CH bonds are not part of the chromophore in SERS-CT. This particular feature of the CH stretching modes makes them quite a suitable reference to show the contribution of the CT mechanism in the remaining vibrations. If the intensity of this $\nu(\text{CH})$ fundamental is used as an internal standard to which the relative intensities are referred to, then every contribution to the SERS intensity other than the resonant CT process is removed, for instance, the electromagnetic (EM) enhancement contributions or the dependence on the surface coverage, which in turn depends on the electrode potential.

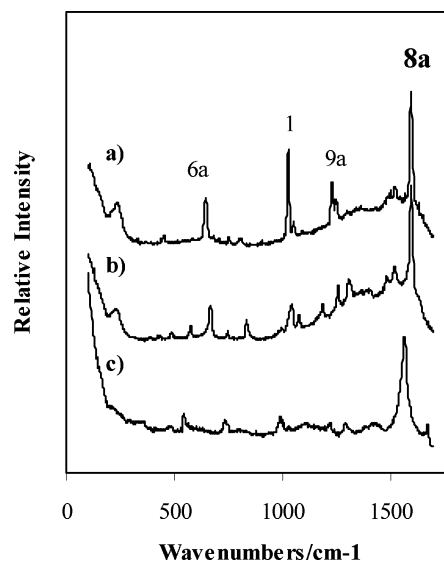


Figure 4. Selected SERS spectra of (a) pyrazine, (b) 2-methylpyrazine, and (c) tetramethylpyrazine recorded on a silver electrode at -0.5 , -0.25 , and -0.75 V, respectively, vs the saturated Ag/AgCl/KCl reference electrode.

Moreover, provided that the $\nu(\text{CH})$ band is an intrinsic internal standard of each adsorbate, all of the other factors influencing the intensities such as surface morphology, degradation, and so forth are removed too. The plots of these relative intensities versus the electrode potential look quite similar to the REP, so we called them SERS-CT profiles^{4d,5} and they allow us to visualize the electronic CT bands, which are quite difficult to observe directly.⁹ Furthermore, the mentioned features are common to the aromatic CH bonds ($\nu(\text{CH})$) of pyridine^{4b} or pyrazine⁵ and the methyl CH bonds ($\nu_s(\text{CH}_3)$) of methyl derivatives,^{4c,d} which allows us to compare the results through this series of molecules.

Although the number of totally symmetric modes of methylpyrazines increases as methylation proceeds, it is observed that only mode $8a; \nu_{\text{ring}}$ exhibits a noticeable SERS enhancement, as can be seen in Figure 4b and c for a low-symmetry molecule such as 2-methylpyrazine (C_s)^{4d} and for an intermediate-symmetry molecule with a high number of atoms such as tetramethylpyrazine (D_{2h}). The totally symmetric modes of these two methyl derivatives amount to 10 and 22, respectively, but the SERS records are always exclusively dominated by the strong band assigned to mode $8a$. This particular vibration is the only totally symmetric fundamental that maintains its frequency and potential energy distribution (PED) along the whole series of studied molecules; on the contrary, the remaining totally symmetric modes are sensitive to the substituents, as in the case of benzene and its derivatives.²⁰ Mode $8a$ shows a very stable frequency, close to 1600 cm^{-1} in all cases, as well as a PED description showing always ca. 65% of ν_{ring} coordinates.^{4,5} These ν_{ring} coordinates are the ones related to the differences between the structures of the neutral molecules and their anions because the transferred electron is located in the LUMO of the adsorbate, allowing the lengthening of the CN bonds and the shortening of the CC bonds as seen in Figure 5a.⁵ That distortion is quite similar to the one originating in mode $8a$ ²¹ (Figure 5b). Provided that no atomic orbital involving hydrogen participates in the LUMO, it is evident that $\nu(\text{CH})$ or $\nu_s(\text{CH}_3)$ vibrations are not perturbed by the CT mechanism, which allows us to taking them as a reference to plot the SERS-CT relative intensities.

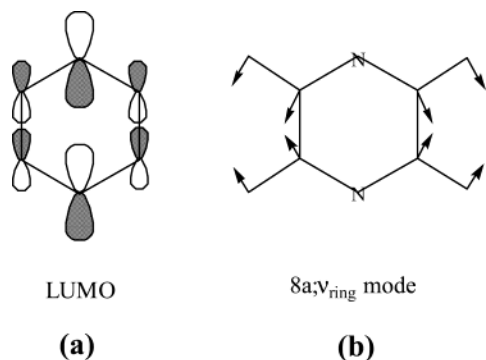


Figure 5. Pictorial plots of (a) the LUMO orbital and (b) mode 8a of pyrazine.

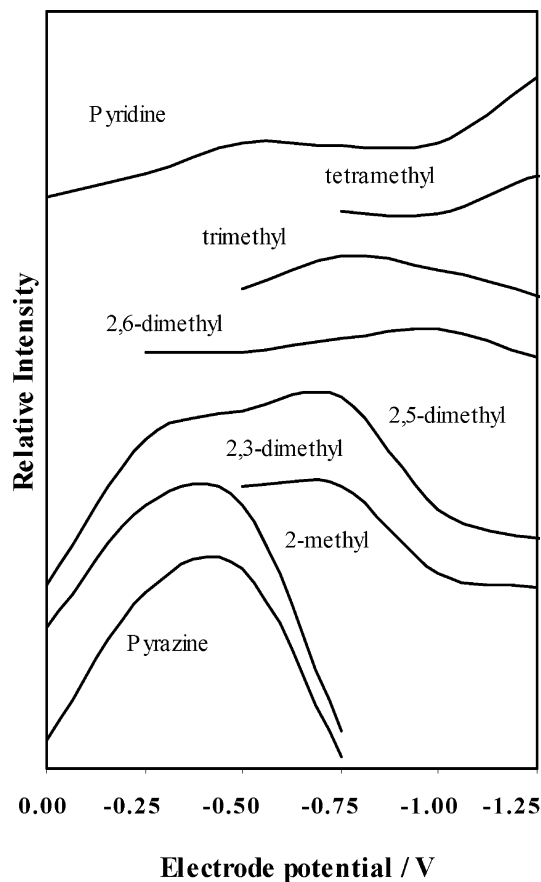


Figure 6. Relative intensities of mode 8a of pyrazine, methylpyrazines, and pyridine recorded in SERS at different electrode potentials with respect to the intensities of the CH stretching bands.

Figure 6 shows the relative intensities of the 8a mode in pyrazine and methylpyrazines with respect to the bands assigned to $\nu(\text{CH})$ and $\nu_s(\text{CH}_3)$, respectively. The intensities have been determined as the heights of the bands in the SERS records. At the bottom of Figure 6, one can see that in the case of pyrazine the maximum appears at $V_{\text{max}} = -0.5$ V, which corresponds to the maximum of the electronic CT band. The SERS-CT profiles of methylpyrazines are vertically offset to make the comparison between them easier. Although the observed patterns become more complex as the number of substituent increases, a general overview shows that the maximum is shifted toward more negative electrode potentials as the number of substituent increases; methylpyrazine shows its maximum at a potential similar to that of pyrazine, -0.5 V; 2,3- and 2,5-dimethyl- and trimethylpyrazine show their maxima at -0.75 V, and 2,6-dimethyl- and tetramethylpyrazine show their maximum values

TABLE 2: Calculated HF/6-31++G Vertical Transitions ($E_{\text{ver}}(\text{D}_0 - \text{S}_0)$) between the Neutral Molecules (S_0 State: Restricted Calculations) and Their Respective Radical Anions (D_0 State: Unrestricted Calculations) and Electrode Potentials Corresponding to the Observed Maxima of the SERS-CT Profiles of Mode 8a (V_{max})^a

molecule	state		$E_{\text{ver}}(\text{D}_0 - \text{S}_0)$ eV	V_{max} V
	S_0	D_0		
pyrazine	$^1\text{A}_g$	$^2\text{B}_{3u}$	0.99	-0.50
2-methyl	$^1\text{A}'$	$^2\text{A}''$	1.07 (0.08)	-0.50 (0.0)
2,3-dimethyl	$^1\text{A}_1$	$^2\text{B}_1$	1.30 (0.31)	-0.75 (-0.25)
2,5-dimethyl	$^1\text{A}_g$	$^2\text{A}_u$	1.13 (0.14)	-0.75 (-0.25)
2,6-dimethyl	$^1\text{A}_1$	$^2\text{B}_1$	1.14 (0.15)	-1.00 (-0.5)
trimethyl	$^1\text{A}'$	$^2\text{A}''$	1.35 (0.36)	-0.75 (-0.25)
tetramethyl	$^1\text{A}_g$	$^2\text{B}_{3u}$	1.56 (0.57)	$-1.25?$ (-0.75)
pyridine	$^1\text{A}_1$	$^2\text{B}_1$	1.80 (0.81)	$-1.25?$ (-0.75)

^a Relative values with respect to pyrazine results are given in parentheses.

at -1.0 and -1.25 V, respectively. Thus, the largest observed shift of the maximum amounts to approximately -1.0 V along this series of molecules. This general trend agrees with the observed behavior of the anions of benzene and its alkyl derivatives in solution as derived from electron-spin resonance (ESR) spectra,²² given that the alkyl substitution destabilizes the radical anion in both series of molecules, but the correlation is not trivial. For instance, every dimethylbenzene shows different electron affinity,²² as dimethylpyrazines do in the respective SERS-CT profiles.

Table 2 summarizes the observed maxima of the SERS-CT profiles (V_{max}) and the ab initio calculated vertical energies between the neutral molecules in the S_0 state and their respective radical anions in the D_0 state ($E_{\text{ver}}(\text{D}_0 - \text{S}_0)$). These results are also summarized in parentheses and are referenced to the values of pyrazine. The HF calculations point out as a general result that successive methylation makes the radical anion less stable. It is foreseen that the relative stability of the radical anion of 2-methylpyrazine should be similar to that of pyrazine, which explains that both molecules show quite similar profiles. One can deduce that 2,3-dimethyl- and trimethylpyrazine should exhibit their maxima shifted some -0.3 or -0.35 V with respect to the maximum of pyrazine, in good agreement with the observed experimental values of -0.25 V. In the cases of 2,5- and 2,6-dimethylpyrazine, the agreement is slightly worse; the experimental shifts amount to -0.25 and -0.5 V, respectively, and the calculated values amount to ca. 0.15 V. Finally, the SERS-CT profile of tetramethylpyrazine does not show any maximum before hydrogen evolution starts. The calculations predict for this molecule a shift amounting to -0.57 V with respect to pyrazine. In any case, the theoretical results foresee that tetramethylpyrazine must show a profile with its maximum more shifted toward negative electrode potentials than any other methyl derivative and that the range of electrode potentials where any maximum is to be expected is on the order of -0.6 V with respect to the case of pyrazine, which is always in good agreement with the experimental behavior.

Figure 6 also includes the SERS-CT profile of mode 8a of pyridine with respect to the $\nu(\text{CH})$ mode as in pyrazine. One can see that no maximum is clearly recorded, as occurs in tetramethylpyrazine. The ab initio computed vertical transition explains why the SERS-CT profiles of pyridine and tetramethylpyridine are quite similar and why the features of the SERS-CT mechanism are observed at much more negative electrode potentials than in pyrazine.^{4a,5} This well-differentiated behavior between the SERS-CT characteristics of pyridine and pyrazine is closely related to the stability of the respective

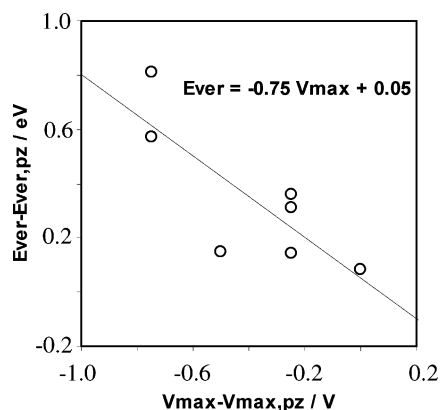


Figure 7. Correlation between the maxima of the SERS-CT profiles ($V_{\max} - V_{\max,pz}$) vs the HF/6-31++G calculated vertical transitions ($E_{\text{ver}} - E_{\text{ver,pz}}$) of pyridine and methylpyrazines with respect to the pyrazine (pz) results.

LUMO as well as to the corresponding electron affinities⁶ ($\Delta E_A = 1$ eV from Table 1).

In Figure 7, the calculated vertical transitions ($E_{\text{ver}} - E_{\text{ver,pz}}$) of pyridine and methylpyrazines are plotted versus the maxima of the SERS-CT profiles ($V_{\max} - V_{\max,pz}$) with respect to the pyrazine (pz) results. The slope in Figure 7 is negative, as can be expected when the electron is transferred from the metal to the adsorbate in the CT excited state. According to eq 8, the slope must equal $-e\beta$, which shows a value of $\beta = 0.75$, and then $S = \beta^{-1} = 1.33$. S values in pyridine over a wide range (0.27–3.46)^{10,15} have been reported for different metals by analyzing the effect of the photon energy on the maxima of the electrode potential (eq 4) instead of by studying the electron affinities of several molecules (eq 8). Another main difference with respect to previous work is the SERS band selected to derive S or β . In this work, we have studied the profiles of mode 8a, which is enhanced exclusively through the CT mechanism; in refs 10 and 15, the profiles of mode 1 were used, but this fundamental can be enhanced through both EM and CT mechanisms.^{4b,e} The β value of 0.75 points out that the effectiveness of the electrode potential in shifting the energy of the CT state is quite sound. The linear dependence of the potential on the distance to the metal surface plotted in Figure 1 corresponds to the Helmholtz model.²³ In actual interphases, β may be not constant and may depend in a complex way on the electrode potential, mainly at potentials more positive than that of zero charge, when the selective adsorption of some anions is favored. However, the Helmholtz model (linear decay of the potential, β is constant, etc.) is more realistic at high electrolyte concentrations, which are the experimental conditions for recording the SERS. Under such conditions, the double layer is more compact: $\beta \rightarrow 1$ given that $\delta \rightarrow z$.

Finally, the general trend of the found correlation can be seen in Figure 8, which shows the effect of methyl substitution on the electrode potentials of the maxima of the SERS-CT profiles (V_{\max}) as well as on the calculated $E_{\text{ver}}(D_0 - S_0)$ at the HF/6-31++G level in pyrazine and its methyl derivatives.

Conclusions

Three singular features allowed us to establish a correlation between the SERS-CT profiles of pyrazine, methylpyrazines, and pyridine. First, in all cases mode 8a plays a singular role in the CT process given that it is by far the most enhanced vibration in this mechanism; it reaches a very strong intensity in all of the SERS records, but it is very weak in the Raman of

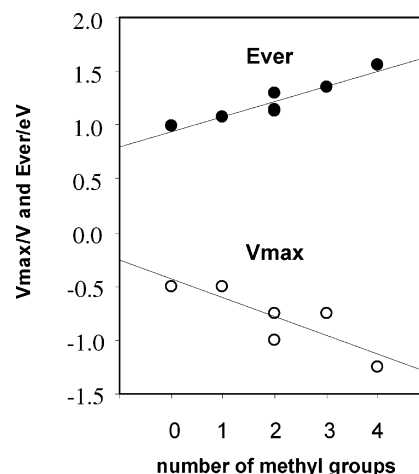


Figure 8. Effect of methyl substitution on the electrode potentials of the maxima of the SERS-CT profiles (V_{\max} , \circ) and on the vertical transitions ($E_{\text{ver}}(D_0 - S_0)$, \bullet) between the D_0 and S_0 states calculated at the HF/6-31++G level in pyrazine and methylpyrazines.

pure samples or their aqueous solutions. Second, mode 8a is almost unaffected by methyl substitution, which makes it easy to assign, appearing as that of the higher frequency in the middle region of the vibrational spectra of the molecules studied here. It can be established that its enhancement is a characteristic feature of the SERS-CT mechanism in aromatic molecules, and this explain why that mode is very strong in many of the previously published papers on SERS. Third, mode $\nu(\text{CH})$ in turn plays the role of internal standard in plots of the SERS-CT profiles. From these profiles, it can be established that methyl substitution makes the radical anion less stable,²⁴ in agreement with the ab initio computed energies of neutral molecules and their respective anions.

Pyrazine and its methyl derivatives are a very advantageous group of molecules because methylation slightly destabilizes the resonant CT state in such a way that they come into the range of available electrode potentials in aqueous solutions. Therefore, the data in Table 2 or Figure 7 can be used to predict the presence of the CT mechanism in the SERS of molecules other than those studied here from the computed ab initio energies of the radical anion with respect to the neutral molecule. Finally, the obtained results confirm the importance of the CT mechanism in SERS³ and the usefulness of these spectra to the understanding of CT processes and to the study of doublet states of the adsorbate, given that its properties in the transient CT levels should be very similar to those of the radical anions of these neutral aromatic molecules.

Acknowledgment. This work was supported by the Spanish MCYT through project BQU2000-1353.

References and Notes

- (1) Creighton, J. A. The Selection Rules for Surface-Enhanced Raman Spectroscopy. In *Spectroscopy of Surfaces*; Clark, R. J. H., Hester, R. E., Eds.; Wiley: Chichester, England, 1988 and references therein.
- (2) Moskovits, M. *Rev. Mod. Phys.* **1985**, *57*, 783.
- (3) See, for instance, Otto, A.; Mrozek, I.; Grabhorn, H.; Akemann, W. *J. Phys.: Condens. Matter* **1992**, *4*, 1143.
- (4) (a) Arenas, J. F.; Woolley, M. S.; Otero, J. C.; Marcos, J. I. *J. Phys. Chem.* **1996**, *100*, 3199. (b) Arenas, J. F.; López Tocón, I.; Otero, J. C.; Marcos, J. I. *J. Phys. Chem.* **1996**, *100*, 9254. (c) Arenas, J. F.; López Tocón, I.; Woolley, M. S.; Otero, J. C.; Marcos, J. I. *J. Raman Spectrosc.* **1998**, *29*, 673. (d) Arenas, J. F.; López Tocón, I.; Otero, J. C.; Marcos, J. I. *Vib. Spectrosc.* **1999**, *19*, 213. (e) López-Tocón, I.; Centeno, S. P.; Otero, J. C.; Marcos, J. I. *J. Mol. Struct.* **2001**, *565–566*, 369. (f) Arenas, J. F.; López Tocón, I.; Centeno, S. P.; Soto, J.; Otero, J. C. *Vib. Spectrosc.* **2002**, *29*, 147. (g) Arenas, J. F.; Otero, J. C.; Centeno, S. P.; López-Tocón, I.

- Soto, J. *Surf. Sci.* **2002**, 511, 163. (h) López-Tocón, I.; Centeno, S. P.; Castro, J. L.; López-Ramírez, M. R.; Otero, J. C. *Chem. Phys. Lett.* **2003**, 377, 111.
- (5) Arenas, J. F.; Woolley, M. S.; López Tocón, I.; Otero, J. C.; Marcos, J. I. *J. Chem. Phys.* **2000**, 112, 7669.
- (6) Nenner, I.; Schulz, G. J. *J. Chem. Phys.* **1975**, 62, 1747.
- (7) Frisch, M. J.; Trucks, G. W.; Schlegel, H. B.; Gill, P. M. W.; Johnson, B. G.; Robb, M. A.; Cheeseman, J. R.; Keith, T.; Petersson, G. A.; Montgomery, J. A.; Raghavachari, K.; Al-Laham, M. A.; Zakrzewski, V. G.; Ortiz, J. V.; Foresman, J. B.; Cioslowski, J.; Stefanov, B. B.; Nanayakkara, A.; Challacombe, M.; Peng, C. Y.; Ayala, P. Y.; Chen, W.; Wong, M. W.; Andres, J. L.; Replogle, E. S.; Gomperts, R.; Martin, R. L.; Fox, D. J.; Binkley, J. S.; Defrees, D. J.; Baker, J.; Stewart, J. P.; Head-Gordon, M.; Gonzalez, C.; Pople, J. A. *Gaussian 94*, revision E.2; Gaussian, Inc.: Pittsburgh, PA, 1995.
- (8) Clark, R. J. H.; Dines, T. J. *Angew. Chem., Int. Ed. Engl.* **1986**, 25, 131.
- (9) See, for instance, (a) Avouris, Ph.; Demuth, J. E. *J. Chem. Phys.* **1981**, 75, 4783. (b) Schmeisser, D.; Demuth, J. E.; Avouris, Ph. *Chem. Phys. Lett.* **1982**, 87, 324. (c) Avouris, Ph.; Demuth, J. E. *Annu. Rev. Phys. Chem.* **1984**, 35, 49. (d) Yamada, H.; Toba, K.; Nakao, Y. *J. Electron Spectrosc. Relat. Phenom.* **1987**, 45, 113. (e) Yamada, H.; Nagaka, H.; Toba, K.; Nakao, Y. *Surf. Sci.* **1987**, 182, 269. (f) Campion, A.; Ivanecky, J. E.; Child, C. M.; Foster, M. *J. Am. Chem. Soc.* **1995**, 117, 11807.
- (10) Lombardi, J. R.; Birke, R. L.; Sanchez, L. A.; Bernard, I.; Sun, S. C. *Chem. Phys. Lett.* **1984**, 104, 240.
- (11) (a) Soto, J.; Fernández, D. J.; Centeno, S. P.; López-Tocón, I.; Otero, J. C. *Langmuir* **2002**, 18, 3100. (b) In this work, ab initio calculations for the Ag^+ -pyrazine, Ag_3^+ -pyrazine, Ag_2 -pyrazine, and Ag_3^- -pyrazine systems have been carried out to simulate the effect of the electrode potential on the observed SERS frequencies. The theoretical and experimental behaviors are in good agreement, indicating that the adsorbed species (A) in the surface complex (M-A) is very similar to the adsorbate in its electronic ground state (A; S_0) at any electrode potential.
- (12) Brolo, A. G.; Irish, D. E. *Z. Naturforsch.* **1995**, 50, 274.
- (13) (a) Arenas, J. F.; Soto, J.; López-Tocón, I.; Fernández, D. J.; Otero, J. C.; Marcos, J. I. *J. Chem. Phys.* **2002**, 116, 7207. (b) This work reports the ab initio results for the Ag_2 -pyrazine system in the ground state ($\text{M}-\text{A}$: S_0 ; A_1) and, amongst others, in the first CT excited level (M^+-A^- : CT_0 ; B_1) of the C_{2v} surface complex. Geometries and vibrational frequencies of pyrazine in this CT state of the complex correlate very well with the calculated parameters for the radical anion in its electronic ground state (A^- : D_0 ; B_{30}). This means that the radical anion of pyrazine has a similar structure to the adsorbate in the CT level of the complex. Yet our unpublished results concerning Ag^+ -pyrazine, Ag_3^+ -pyrazine and Ag_3^- -pyrazine systems extend this conclusion to any electrode potential.
- (14) Avouris, Ph.; Persson, N. J. *J. Phys. Chem.* **1984**, 88, 837.
- (15) (a) Tian, Z. Q.; Ren, B.; Wu, D. *J. Phys. Chem. B* **2002**, 106, 9463. (b) Kudelski, A.; Bukowska, J. *J. Raman Spectrosc.* **1994**, 222, 555 and references therein.
- (16) A similar hypothesis is made in ref 6 to compare experimental electron affinities in the gas phase with polarographic potentials of different molecules.
- (17) See, for instance, Heinrich, N.; Koch, W.; Frenking, G. *Chem. Phys. Lett.* **1986**, 124, 20 and references therein.
- (18) (a) Creighton, J. A. *Surf. Sci.* **1985**, 158, 211. (b) Creighton, J. A. *Surf. Sci.* **1986**, 173, 665.
- (19) (a) Hirakawa, A. Y.; Tsuboi, M. *Science* **1975**, 188, 359. (b) Strommen, D. P.; Nakamoto, K. *J. Chem. Educ.* **1977**, 54, 474.
- (20) Varsanyi, G. *Vibrational Spectra of Benzene Derivatives*; Academic Press: New York, 1969.
- (21) McDonald, D. B.; Rice, S. A. *J. Chem. Phys.* **1981**, 74, 4893.
- (22) Jordan, K. D.; Michejda, J. A.; Burrow, P. D. *J. Am. Chem. Soc.* **1976**, 98, 1295 and references therein.
- (23) Brett, C. M. A.; Brett, A. M. O. *Electrochemistry: Principles, Methods and Applications*; Oxford University Press: Oxford, England, 1993.
- (24) This result is rationalized by "the electron release by the alkyl groups to the ring."²²